UCLA
UCLA Previously Published Works

Title

Diffusion MRI is an early biomarker of overall survival benefit in IDH wild-type recurrent glioblastoma treated with immune checkpoint inhibitors

Permalink

https://escholarship.org/uc/item/3236b823

Journal

Neuro-Oncology, 24(6)

ISSN

1522-8517

Authors

Hagiwara, Akifumi

Oughourlian, Talia C

Cho, Nicholas S

et al.

Publication Date

2022-06-01

DOI

10.1093/neuonc/noab276

Peer reviewed

Neuro-Oncology

Diffusion MRI is an early biomarker of overall survival benefit in IDH wild-type recurrent glioblastoma treated with immune checkpoint inhibitors

Akifumi Hagiwara[ORCID]**, Talia C. Oughourlian, Nicholas S. Cho, Jacob Schlossman, Chencai Wang, Jingwen Yao, Catalina Raymond, Richard Everson, Kunal Patel, Sergey Mareninov, Fausto J. Rodriguez, Noriko Salamon, Whitney B. Pope, Phioanh L. Nghiemphu, Linda M. Liau**[ORCID]**, Robert M. Prins, Timothy F. Cloughesy**[ORCID]**, and Benjamin M. Ellingson**[ORCID]

UCLA Brain Tumor Imaging Laboratory (BTIL), Center for Computer Vision and Imaging Biomarkers, University of California, Los Angeles, Los Angeles, California, USA (A.H., T.C.O., N.S.C., J.S., C.W., J.Y., C.R., B.M.E.); Department of Radiological Sciences, David Geffen School of Medicine, University of California, Los Angeles, Los Angeles, California, USA (A.H., T.C.O., N.S.C., J.S., C.W., J.Y., C.R., N.S., W.B.P., B.M.E.); Department of Radiology, Juntendo University School of Medicine, Tokyo, Japan (A.H.); Neuroscience Interdepartmental PhD Program, David Geffen School of Medicine, University of California, Los Angeles, Los Angeles, California, USA (T.C.O.); Department of Bioengineering, Henry Samueli School of Engineering and Applied Science, University of California, Los Angeles, Los Angeles, California, USA (N.S.C., B.M.E.); Medical Scientist Training Program, David Geffen School of Medicine, University of California, Los Angeles, Los Angeles, California, USA (N.S.C.); Department of Neurosurgery, David Geffen School of Medicine, University of California, Los Angeles, Los Angeles, California, USA (R.E., K.P., L.M.L., R.M.P.); Department of Pathology, David Geffen School of Medicine, University of California, Los Angeles, Los Angeles, California, USA (S.M., F.J.R.); UCLA Neuro-Oncology Program, University of California, Los Angeles, Los Angeles, California, USA (P.L.N., T.F.C., B.M.E.); Department of Neurology, David Geffen School of Medicine, University of California, Los Angeles, Los Angeles, California, USA (T.F.C.); Department of Psychiatry and Biobehavioral Sciences, David Geffen School of Medicine, University of California, Los Angeles, Los Angeles, California, USA (B.M.E.)

Corresponding Author: Benjamin M. Ellingson, PhD, Director, UCLA Brain Tumor Imaging Laboratory (BTIL), Professor of Radiology and Psychiatry, Departments of Radiological Sciences and Psychiatry, David Geffen School of Medicine, University of California, Los Angeles, 924 Westwood Blvd., Suite 615, Los Angeles, CA 90024, USA (bellingson@mednet.ucla.edu).

Abstract

Background. Diffusion MRI estimates of the apparent diffusion coefficient (ADC) have been shown to be useful in predicting treatment response in patients with glioblastoma (GBM), with ADC elevations indicating tumor cell death. We aimed to investigate whether the ADC values measured before and after treatment with immune checkpoint inhibitors (ICIs) and the changes in these ADC values could predict overall survival (OS) in patients with recurrent IDH wild-type GBM.

Methods. Forty-four patients who met the following inclusion criteria were included in this retrospective study: (i) diagnosed with recurrent IDH wild-type GBM and treated with either pembrolizumab or nivolumab and (ii) availability of diffusion data on pre- and post-ICI MRI. Tumor volume and the median relative ADC (rADC) with respect to the normal-appearing white matter within the enhancing tumor were calculated.

Results. Median OS among all patients was 8.1 months (range, 1.0–22.5 months). Log-rank test revealed that higher post-treatment rADC was associated with a significantly longer OS (median, 10.3 months for rADC $\geq$ 1.63 versus 6.1 months for rADC < 1.63; $P = .02$), whereas tumor volume, pretreatment rADC, and changes in rADC after treatment were not significantly associated with OS. Cox regression analysis revealed that post-treatment rADC significantly influenced OS ($P = .02$, univariate analysis), even after controlling for age and sex ($P = .01$, multivariate analysis), and additionally controlling for surgery after ICI treatment ($P = .045$, multivariate analysis).

Conclusions. Elevated post-treatment rADC may be an early imaging biomarker for OS benefits in GBM patients receiving ICI treatment.

Key Points

- In recurrent IDH wild-type GBM treated with ICIs, post-treatment rADC was associated with OS.

- This association was significant even after controlling for clinical factors.

Importance of the Study

Although immunotherapies are considered promising therapeutic approaches for GBM, immune checkpoint inhibitors (ICIs) such as pembrolizumab and nivolumab have not demonstrated an OS benefit in patients with GBM, highlighting the need for noninvasive biomarkers to assess treatment response. Results from the current study suggest diffusion MRI may be a valuable early imaging biomarker for recurrent IDH wild-type GBM treated with ICIs, as elevated water diffusivity after treatment was found to be predictive of survival.

Despite advances in pharmacotherapy, radiation, and surgery, the prognosis of patients with isocitrate dehydrogenase (IDH) wild-type glioblastoma (GBM) remains dismal, with median survival intervals of approximately 10–15 months.[1] Due to its aggressive nature, almost all GBMs recur after initial therapy. Immunotherapy is a promising approach for GBM because of its potential to overcome the intrinsic immunosuppressive effects of the disease and those induced by the current standard-of-care treatments, ultimately promoting an antitumor immune response.[2] However, randomized clinical trials of immune checkpoint inhibitors (ICIs), including pembrolizumab and nivolumab, have not demonstrated an overall survival (OS) benefit in patients with recurrent GBM.[3,4] Thus, there is an urgent need to identify noninvasive biomarkers to predict patient response to ICIs and further develop combination therapies to improve patient outcomes.

MRI with and without injection of a contrast agent is the current gold standard for determining the burden of disease in brain tumors[5–7]; however, pseudoprogression is more common after immunotherapy, with reports describing frequent contrast enhancement due to the increased permeability of the blood-brain barrier as a result of the direct and/or indirect effects of immunotherapy.[8] Moreover, prior to a delayed treatment effect, an initial increase in tumor volume due to immune cell infiltration and true progression have been reported in immunotherapy, further complicating evaluations of the treatment effect.[2] Immunotherapy Response Assessment in Neuro-Oncology (iRANO) criteria have recommended that confirmation of progression should occur 6 months after initiation of immunotherapy[9,10]; however, many recurrent GBM patients (~60%) do not survive more than 6 months from initiation of therapy to confirm progression and iRANO-defined progression-free survival (PFS) has not been shown to be valuable for predicting OS.[11] Thus, there remains an unmet clinical need for a noninvasive imaging technique to identify early response to immunotherapies and potentially further our understanding of the biological mechanisms that underly both response and resistance to immunotherapies.

Diffusion-weighted imaging (DWI) measures of the apparent diffusion coefficient (ADC), a metric related to the mobility of water within the tissue microenvironment and inversely proportional to tumor cellularity,[12–14] has shown promise as a predictive and prognostic biomarker in GBM under a variety of therapeutic scenarios and may provide an early indicator of successful immunotherapy. For example, elevated ADC after standard chemoradiotherapy and anti-angiogenic therapy was associated with better PFS and OS,[15–19] and similarly, Song *et al.* recently showed a promising association between ADC and PFS at 6 months after ICI treatment in patients with recurrent GBM.[20] Therefore, we hypothesized that an increase in ADC and/or an elevated ADC following immunotherapy would indicate successful tumor destruction and a more favorable OS. The goal of the current study was to investigate the potential utility of diffusion MRI as an early indicator of favorable OS in patients with recurrent IDH wild-type GBM treated with ICIs.

Materials and Methods

Patient Selection

Patients included in this retrospective study were diagnosed with recurrent IDH wild-type GBM, either by evaluation of surgical pathology before or after the initiation of ICIs or by meeting the definition of recurrent disease using RANO criteria,[7] at least 6 months after the last concurrent treatment with temozolomide and radiotherapy, and were treated with ICIs between April 2014 and July 2021. We included cases with diffusion MRI data before and after standard-dose ICI treatment, if they were not treated with bevacizumab between 3 months prior to the pre-ICI MRI scan and the date of post-ICI MRI scan, because

bevacizumab is known to affect ADC values.[21] Only one pre-ICI and one post-ICI MRI data closest to the date of the initiation of ICI were selected and analyzed for each patient. The treatment included nivolumab administration every 2 weeks and pembrolizumab administration every 3 weeks. The exclusion criteria were as follows: (1) debulking surgery between pre- and post-ICI diffusion MRI and (2) severe MRI artifacts on brain scans. PFS was defined as the time period between the date of initiation of the ICI therapy and the date that tumor recurrence was confirmed using MRI or clinical symptoms as defined by RANO criteria,[7] or censor date. OS was defined as the time period between the date of initiation of the ICI therapy and the date of death for any reason or censor date. This retrospective study was approved by the Institutional Review Board, and the requirement for informed consent was waived.

MR Acquisition

All patients underwent T1-weighted imaging before and after administration of gadolinium-based contrast agent and DWI or diffusion tensor imaging (DTI) at 1.5 T or 3 T with b values of 0 and 1000 s/mm^2 as part of standard of care either at our institution or external institutions. T1-weighted imaging was performed with 2D axial turbo spin echo with a 5-mm slice thickness and 1–1.5 mm gap or a 3-mm slice thickness and no interslice gap or using a 3D inversion-prepared gradient echo with a 1–1.5-mm isotropic voxel size. At 1.5 T, DWI using a single-shot echo-planar sequence was performed with the following parameters: TE/TR = 74–109/5800–10 000 ms, pixel size = 0.94 mm × 0.94 mm–1.88 mm × 1.88 mm, slice thickness = 3–5 mm with an interslice gap of 0–1 mm. At 3T, DWI using a single-shot echo-planar sequence or DTI along 64 motion-probing gradients was performed with the following parameters: TE/TR = 66–100/4000–11 500 ms, pixel size = 2 mm × 2 mm, slice thickness = 2–4 mm with no interslice gap for DTI; TE/TR = 73–112/5700–10 000 ms, pixel size = 0.94 mm × 0.94 mm–2 mm × 2 mm, slice thickness = 2–3 mm with an interslice gap of 0–1 mm for DWI. ADC maps were calculated from the DWI and DTI data.

Postprocessing of MRI Data

All MRI images were registered to the postcontrast enhanced T1-weighted images using a six-degree-of-freedom rigid transformation and a mutual information cost function using FSL software (*flirt*; Functional Magnetic Resonance Imaging of the Brain Software Library; Oxford, England) for subsequent analyses.

The volume of interest of the enhancing tumor was defined on contrast-enhanced T1-weighted images by digital subtraction maps using a semi-automated thresholding method[22] with the Analysis of Functional NeuroImages software (NIMH Scientific and Statistical Computing Core). Signal intensity of the contrast-enhanced and noncontrast-enhanced T1-weighted images were normalized before subtraction, so the enhancement showed voxel value of more than 0.1. First, the general enhancing regions of the tumor on postcontrast T1-weighted images were manually defined. Then, T1-weighted subtraction map images were

thresholded at 0.1 to best define the extent of abnormality. Finally, the resulting masks were edited manually by a neuroradiologist with more than 10 years of experience (AH) to exclude large vessels and any obvious non-tumor regions, which typically occupied only minor fractions of the entire region of interest. Because ADC is known to show variability across scanners,[23] relative ADC (rADC) was calculated by normalizing ADC maps by the mean value of normal-appearing white matter in the contralateral hemisphere to reduce variability induced by scanner differences.[20,24] Three spherical volumes of interest, each 5 mm in diameter, were put in the central semiovale in the anterior, middle, and posterior area around 3 mm above the upper end of the lateral ventricles contralateral to the tumor by AH using ITK-SNAP,[25] and these three volumes ions of interest were treated as a single region of interest to extract the mean normal-appearing white matter value (Figure 1). Another investigator (NSC, with 6 years of experience in neuroimaging analysis) independently performed the same procedure for putting volumes of interest on normal-appearing white matter to estimate the interobserver reproducibility of rADC measurement in the tumor. The median rADC was extracted from enhancing tumor volume of interest for further analyses. Notably, although both 1.5 T and 3 T were used in this study, theoretically, ADC is not affected by field strengths.[26]

Statistical Analysis

The intraclass correlation coefficient for median rADC values in the tumor and its 95% confidence interval (CI) were calculated between two observers using a two-way random absolute single measures model. A paired t-test was used to evaluate the differences in tumor volumes, ADC, and rADC before and after ICI treatment. Log-rank tests stratified by median values and univariate Cox regression analysis were performed to assess the effect of tumor volume, ADC, and rADC (pretreatment, post-treatment, and percentage change) as risk factors for PFS and OS. For metrics that showed statistical significance, we optimized the thresholds for differentiating patients with better and worse survival by performing log-rank tests at each incremental point of the metric. The optimal threshold was set such that the P value was the lowest.[27] Additional multivariate Cox regression analysis was performed for OS by including age and sex in the regression model. We also included whether the patient underwent debulking surgery after the initiation of ICI treatment in the model, as this has been shown to significantly alter survival.[28] Statistical significance was set at $P < .05$. Statistical analyses were performed using MATLAB software (version R2018a, Mathworks, Inc.).

Results

Among the 49 patients who met the inclusion criteria, one patient with severe motion artifacts on MRI and four who underwent debulking surgeries between pre- and post-ICI MRI were excluded. Thus, a total of 44 patients (21 males and 23 females) with a mean age of 53.9 ± 12.2 years were
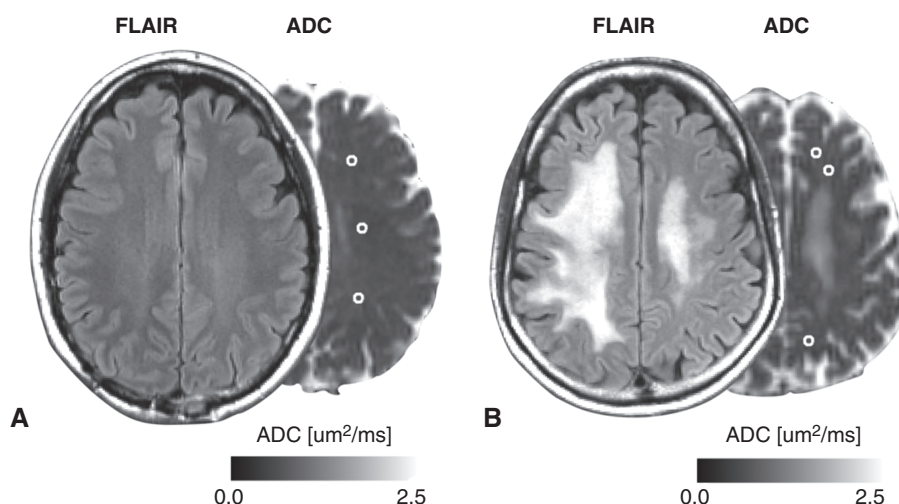
Fig. 1 (A–B) Fluid-attenuated inversion recovery (FLAIR) images and ADC maps of two representative patients with GBM who were treated with ICIs. Volumes of interest in the normal-appearing white matter are outlined in white. These are the post-ICI MRI of the same subjects as shown in Figure 2. Three spherical volumes of interest, 5 mm in diameter, were put in the central semiovale in the anterior, middle, and posterior area around 3 mm above the upper end of the lateral ventricles contralateral to the tumor. (B) because this patient had white matter abnormality in the contralateral central semiovale, volumes-of-interest were put to avoid the abnormality.

included and analyzed. The mean ± standard deviation of the time interval between the pre- and post-ICI MRI studies and between treatment initiation and post-ICI MRI studies were 1.6 ± 1.6 and 0.7 ± 0.5 months, respectively. The median number and range of treatment cycles between pre-ICI and post-ICI MRI were 1 (range, 1–2) for Pembrolizumab and 2 (range, 1–4) for Nivolumab. Additional patient demographics are presented in Supplementary Table 1. The intraclass correlation coefficient between two observers for rADC values in the tumor was 0.97 (95% CI, 0.96–0.98), indicating excellent reproducibility of the measurement.

The median PFS and OS from the start of ICI treatment were 2.7 months (range, 0.6–8.7 months) and 8.1 months (range, 1.0–22.5 months), respectively. Enhancing tumor volume in the post-ICI scan was significantly higher than that in the pre-ICI scan (mean ± standard deviation; 25.4 ± 21.2 mL and 13.9 ± 13.2mL, respectively; $P < .001$). However, ADC in the pre- and post-ICI scans did not show significant differences (mean ± standard deviation; 1262 ± 280 × 10^{-6} mm^2/s and 1275 ± 221 × 10^{-6} mm^2/s, respectively; $P = .73$). rADC in the pre- and post-ICI scans did not show significant differences either (mean ± standard deviation; 1.72 ± 0.34 and 1.68 ± 0.35, respectively; $P = .37$). Figure 2 shows two representative cases demonstrating an increase and decrease in tumor volume and rADC after ICI treatment.

Pre- and post-ICI tumor volume, ADC, and rADC, and percentage change in tumor volume, ADC, and rADC were not significantly associated with PFS using log-rank tests stratifying patients by median measurements.

Patients with a post-ICI rADC value more than 1.63 had a significantly longer OS than those showing smaller rADC values (Figure 3; log-rank, $P = .02$, HR = 0.41; median OS, 10.3 vs. 6.1 months). Pre- and post-ICI tumor volume and ADC, pre-ICI rADC, and percentage change in tumor

volume, ADC, and rADC were not significantly associated with OS using log-rank tests stratifying patients by the median measurement. When we looped through the rADC values with increment of 0.1, thresholding with rADC value of 1.04–1.80 all resulted in significant results, with variable number of patients in groups with better and worse survival. The lowest P value of 1.8×10^{-5} was achieved at rADC 1.43–1.46, grouping 10 patients with worse OS and 34 patients with better OS (Figure 4).

Pre- and post-ICI tumor volume, ADC, and rADC, and percentage change in tumor volume, ADC, and rADC did not show a significant association with PFS using univariate Cox regression analysis (Table 1). Univariate analysis demonstrated a significant association between post-ICI ADC or rADC and OS (Table 2; $P = .02$, HR = 0.998, 95% CI 0.996–1.000 and $P = .006$, HR = 0.22, 95% CI 0.07–0.64, respectively), and pre-ICI ADC or rADC was also associated with OS (Table 2; $P = .04$, HR = 0.999, 95% CI 0.997–1.000 and $P = .01$, HR = 0.22, 95% CI 0.07–0.70, respectively), but other metrics were not found to be associated with OS. Age was significantly associated with OS (Supplementary Table 2; $P = .04$, HR = 1.028, 95% CI 1.001–1.055), whereas sex and whether the patient underwent debulking surgery after the initiation of ICI treatment were not associated with OS (Supplementary Table 2).

When controlling for age and sex, post-ICI ADC, post-ICI rADC, and pre-ICI rADC were significantly associated with OS (Table 2; $P = .03$, HR = 0.998, 95% CI 0.996–1.000 for post-ICI ADC; $P = .01$, HR = 0.24, 95% CI 0.07–0.75 for post-ICI rADC; and $P = .04$, HR = 0.26, 95% CI 0.07–0.91 for pre-ICI rADC). Moreover, post-ICI rADC was significantly associated with OS even after additionally controlling for whether debulking surgery was performed sometime after ICI treatment (Table 2; $P = .045$, HR = 0.29, 95% CI 0.08–0.98),
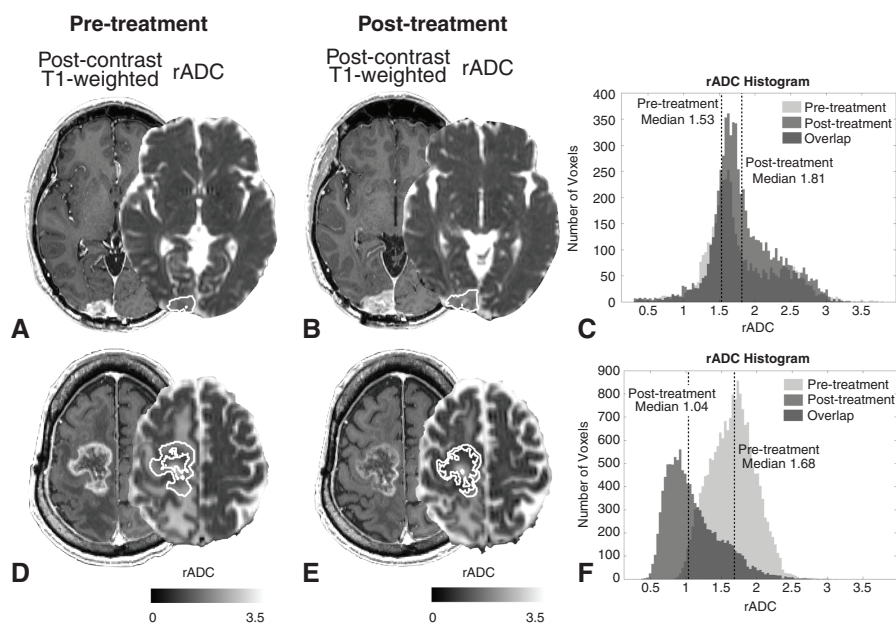
Fig. 2 Postcontrast T1-weighted images and rADC maps of two representative patients with GBM who were treated with ICIs. Contrast-enhancing tumor volumes of interest are outlined in white. (A–C) The (A) pre- and (B) postscans of a 51-year-old male patient who showed an increase in both tumor volume and median rADC after ICI treatment (+73.2% and +8.9%, respectively; rADC histograms are shown in (C)). Although the tumor volume increased after treatment, the patient's post-treatment rADC was relatively high (1.81) and OS was long (22.5 months). (D–F) The (D) pre- and (E) postscans of a 65-year-old male patient who showed a decrease in both tumor volume and median rADC after ICI treatment (-37.6% and -38.2%, respectively; rADC histograms are shown in (F)). Although the tumor volume decreased after treatment, the patient's post-treatment rADC was relatively low (1.01) and OS was short (1.0 month).
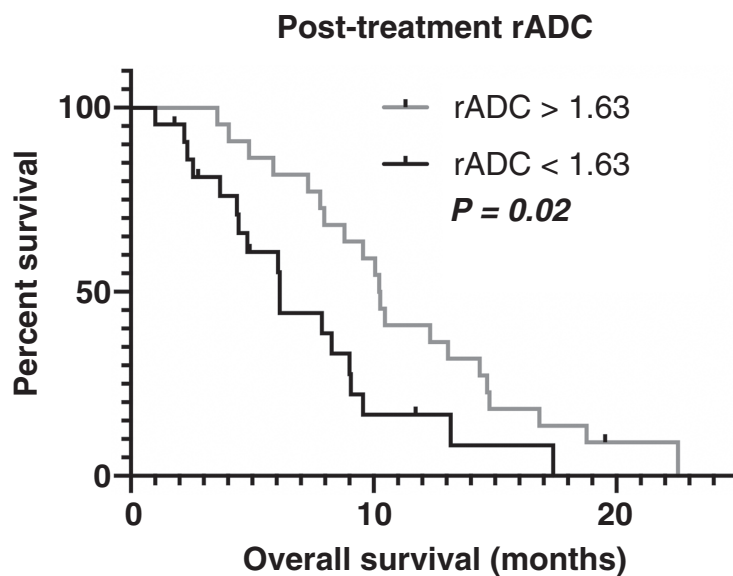

Fig. 3 Comparison of OS between groups stratified by median values of post-ICI rADC. Kaplan–Meier plot shows higher OS in GBM with post-treatment rADC > 1.63 (C, log-rank, P = .02). Other comparisons did not show a statistically significant difference.
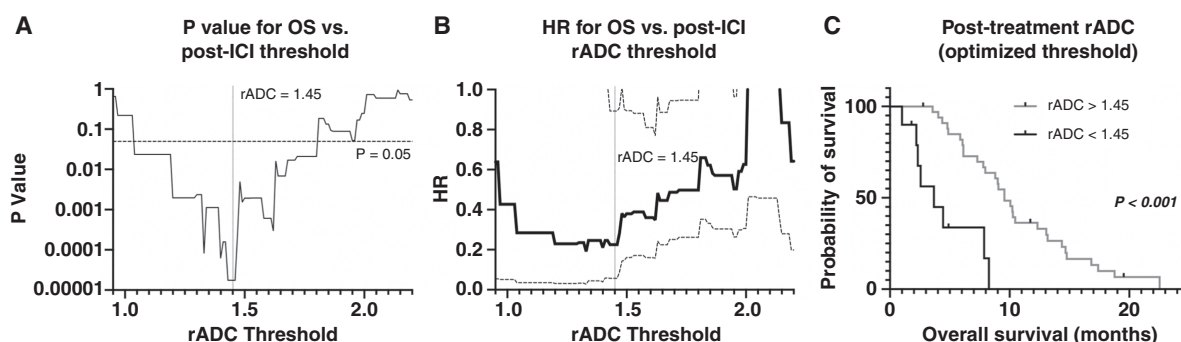
Fig. 4 (A) Level of significance (*P* values) for OS differences for different rADC thresholds at post-ICI time point investigated with log-rank analysis. The lowest *P* value of 1.8×10^{-5} was achieved at rADC 1.43–1.46. (B) Hazard ratios (HRs, lower rADC as reference, solid black line) and 95% confidence intervals (dashed lines) for OS in recurrent GBM for different rADC thresholds. (C) Kaplan–Meier plot shows higher OS in GBM with post-treatment rADC > 1.45.

Table 1 Univariate Cox Regression Analysis of PFS

	PFS (Univariate)		
	P value	*z*-score	HR (95%CI)
Volume			
Pre-ICIs	.90	−0.13	0.999 (0.979–1.019)
Post-ICIs	.87	0.16	1.001 (0.988–1.015)
Percentage change	.40	−0.84	1.000 (0.999–1.000)
ADC			
Pre-ICIs	.68	−0.42	1.000 (0.998–1.001)
Post-ICIs	.31	−1.01	0.999 (0.998–1.001)
Percentage change	.93	−0.09	0.999 (0.999–1.000)
rADC			
Pre-ICIs	.06	−1.88	0.34 (0.11–1.04)
Post-ICIs	.16	−1.41	0.54 (0.23–1.27)
Percentage change	.60	0.52	1.003 (0.990–1.018)

whereas post-ICI ADC and pre-ICI rADC were not significantly associated with OS (Table 2; *P* = .07, HR = 0.998, 95% CI 0.996–1.000 for post-ICI ADC; and *P* = .07, HR = 0.30, 95% CI 0.08–1.08 for pre-ICI rADC).

Discussion

Selection of optimal therapies for GBM patients and identifying early treatment response or failure remains some of the most challenging issues in clinical neuro-oncology. Identifying successful response and early failure to immunotherapies, in particular, remains puzzling and problematic. The results of the present study appear to suggest that diffusion MRI may be a valuable imaging approach for understanding treatment response to immunotherapies in GBM. In particular, results suggest elevated rADC within the enhancing tumor after ICI treatment is a

significant predictor of OS benefit in GBM. Even after controlling for known clinical prognostic factors, rADC within the enhancing tumor after ICI treatment remained a strong predictor of OS in GBM. Together, this suggests diffusion MRI may serve as an early noninvasive biomarker for prediction of successful ICI therapy in GBM. Notably, tumor volume was not significantly associated with OS, while rADC was associated with OS. This may exemplify the potential implication of inclusion of advanced MR imaging technique such as DWI into the RANO criteria in the future.

In contrast to the findings of a previous study examining GBM response to ICI therapy,[20] we did not observe a significant association between diffusion MRI measurements and PFS. This may be due to the fact that the previous study utilized the iRANO criteria for determination of PFS, whereas in the current study we used the conventional RANO criteria, as many patients died before reaching the 6 month confirmation time point. Nonetheless, our study does support the hypothesis that diffusion MRI changes

Table 2 Univariate and Multivariate Cox Regression Analysis of OS

	OS (Univariate)			OS (Multivariate)[a]			OS (Multivariate)[b]		
	P value	*z*-score	HR (95%CI)	*P* value	*z*-score	HR (95%CI)	*P* value	*z*-score	HR (95%CI)
Volume									
Pre-ICIs	.47	0.72	1.008 (0.986–1.032)	.84	0.21	1.002 (0.979–1.026)	.41	0.83	1.010 (0.986–1.036)
Post-ICIs	.17	1.38	1.012 (0.995–1.029)	.29	1.06	1.009 (0.992–1.027)	.13	1.53	1.014 (0.996–1.031)
Percentage change	.99	−0.01	1.000 (1.000–1.000)	.74	0.34	1.000 (1.000–1.000)	.51	0.66	1.000 (1.000–1.001)
ADC									
Pre-ICIs	.04*	−2.01	0.999 (0.997–1.000)	.08	−1.75	0.999 (0.997–1.000)	.11	−1.60	0.999 (0.997–1.000)
Post-ICIs	.02*	−2.26	0.998 (0.996–1.000)	.03*	−2.15	0.998 (0.996–1.000)	.07	−1.81	0.998 (0.996–1.000)
Percentage change	.24	1.16	1.009 (0.994–1.024)	.31	1.02	1.009 (0.992–1.025)	.23	1.20	1.010 (0.994–1.027)
rADC									
Pre-ICIs	.01*	−2.57	0.22 (0.07–0.70)	.04*	−2.11	0.26 (0.07–0.91)	.07	−1.84	0.30 (0.08–1.08)
Post-ICIs	.006**	−2.75	0.22 (0.07–0.64)	.01*	−2.44	0.24 (0.07–0.75)	.045*	−2.00	0.29 (0.08–0.98)
Percentage change	.20	1.30	1.014 (0.993–1.036)	.22	1.23	1.015 (0.992–1.038)	.15	1.43	1.016 (0.994–1.038)

[a]Controlling for age and sex.
[b]Controlling for age, sex, and whether a patient underwent surgery after the initiation of ICIs treatment. *$P < 0.05$, **$P < .01$.

after ICI treatment may be early predictors of successful therapy in GBM.

We theorize the association between higher ADC and better survival may be related to higher rates of tumor cell death, because ADC has been shown to be inversely correlated with tumor cell density in a number of studies.[12–14,29,30] However, the biological implications of ADC in the context of immunotherapy may have additional significance, since response to immunotherapy can be delayed compared to conventional chemoradiotherapy.[9] In a recent study, the mean value of the lower peak of the ADC histogram in GBM was revealed to be positively correlated with the expression of decorin, a small proteoglycan belonging to the small leucine-rich proteoglycan family that alters the viscosity of the extracellular matrix.[31] Decorin softens the extracellular matrix by binding with various macromolecules and activating specific matrix metalloproteinases,[32] which may partly explain the relationship between increased decorin expression and increased ADC, a measure of water mobility (or viscosity) within tissues. Extracellular matrix remodeling has recently been revealed to play a crucial role in immune cell activation and trafficking and immunological synapse formation.[33] Moreover, in addition to decorin, other molecules in the small leucine-rich proteoglycan family are capable of binding to toll-like receptors, complement C1q, and tumor necrosis factor-alpha, leading to regulation of innate immunity and inflammation.[34] Thus, studies aimed at identifying causal associations between ADC, efficacy of immunotherapy, and molecular mechanisms are still warranted.

In this study, post-ICI rADC was significantly associated with OS by log-rank test and Cox regression analysis

after controlling for age, sex, and whether the patient underwent debulking surgery after the initiation of ICI treatment, whereas raw ADC was not significantly associated with OS with the same analyses. Only a handful of studies have compared the utility of rADC and ADC in high-grade gliomas. Elson et al.[35] and Gutierrez et al.[36] showed benefit of rADC over ADC in predicting survival and treatment response, respectively, whereas Qin et al.[37] did not find obvious difference between rADC and ADC in their association with 15-month OS after surgery. Our study has further demonstrated the advantage of rADC over ADC.

The current study has some limitations that should be addressed. First, because of the retrospective nature of this study, the timing and acquisition protocol for pre-and post-treatment imaging was not well controlled. We decided to analyze the first post-ICI scan data rather than setting a certain timing criterion because some patients underwent debulking surgery right after the first post-ICI scan. Future, prospective studies that control for these technical and logistical factors should be performed to confirm our findings in a larger cohort of patients. We mitigated these issues partially by normalizing tumor measurements with contralateral normal-appearing white matter, but this may not be sufficient. Second, we did not investigate temporal trends in ADC and tumor volumes after the initiation of ICI treatment in this study. Further studies should examine temporal trends in ADC and volumetric changes to see if they provide additional insights into their associations with survival. Third, even though we investigated the patients treated with pembrolizumab and nivolumab, some cases were treated concurrently with other treatments, including immunotherapies such as ipilimumab and tasadenoturev,

between pre-ICI and post-ICI MRI time points. These treatments may have affected ADC values, though we already excluded patients treated concurrently or recently with bevacizumab, which is widely known to affect ADC values.[21] Even though the results of the current study may be potentially applicable to other immunotherapies, this should be investigated in the future. Lastly, even though pseudoprogression typically occurs within 6 months after concurrent temozolomide and radiotherapy, it could occur even after 6 months and radiation necrosis may occur several years after treatment,[38] and these possibilities were not fully excluded in our cohort upon inclusion in the current study.

Conclusions

Results from the current study suggest that elevated ADC within the enhancing tumor predicts favorable survival in GBM patients treated with immune checkpoint inhibitors. Results support the hypothesis that diffusion MRI may be a valuable early imaging biomarker for successful immunotherapy in GBM.

Supplementary Material

Supplementary material is available at *Neuro-Oncology* online.

Keywords

ADC | ICI | IDH wild type | MRI | recurrent glioblastoma

Conflict of interest statement. BME is on advisory board of Hoffman La-Roche, Siemens, Nativis, Medicenna, MedQIA, Bristol Meyers Squibb, Imaging Endpoints, and Agios. BME is a paid consultant of Nativis, MedQIA, Siemens, Hoffman La-Roche, Imaging Endpoints, Medicenna, and Agios. BME has grant funding by Hoffman La-Roche, Siemens, Agios, and Janssen. The other authors declare no competing interests.

Authorship statement. Study design: A.H., B.M.E. Data collection: A.H., T.C.O., N.S.C., J.S., C.W., J.Y., C.R., R.E., K.P., S.M.,

W.H.Y., N.S., W.B.P., P.L.N., L.M.L., R.M.P., T.F.C. Statistical analysis: A.H., J.Y. Manuscript preparation: A.H., T.C.O., N.S.C., J.S., C.W., J.Y., C.R., R.E., K.P., S.M., W.H.Y., N.S., W.B.P., P.L.N., L.M.L., R.M.P., T.F.C., B.M.E.

References

1. Yan H, Parsons DW, Jin G, et al. IDH1 and IDH2 mutations in gliomas. *N Engl J Med.* 2009;360(8):765–773.
2. Lim M, Xia Y, Bettegowda C, Weller M. Current state of immunotherapy for glioblastoma. *Nat Rev Clin Oncol.* 2018;15(7):422–442.
3. Nayak L, Molinaro AM, Peters K, et al. Randomized phase II and biomarker study of pembrolizumab plus bevacizumab versus pembrolizumab alone for patients with recurrent glioblastoma. *Clin Cancer Res.* 2021;27(4):1048–1057.
4. Reardon DA, Brandes AA, Omuro A, et al. Effect of nivolumab vs bevacizumab in patients with recurrent glioblastoma: the checkmate 143 phase 3 randomized clinical trial. *JAMA Oncol.* 2020;6(7):1003–1010.
5. Bette S, Barz M, Wiestler B, et al. Prognostic value of tumor volume in glioblastoma patients: size also matters for patients with incomplete resection. *Ann Surg Oncol.* 2018;25(2):558–564.
6. Ellingson BM, Abrey LE, Nelson SJ, et al. Validation of postoperative residual contrast-enhancing tumor volume as an independent prognostic factor for overall survival in newly diagnosed glioblastoma. *Neuro Oncol.* 2018;20(9):1240–1250.
7. Wen PY, Macdonald DR, Reardon DA, et al. Updated response assessment criteria for high-grade gliomas: response assessment in neuro-oncology working group. *J Clin Oncol.* 2010;28(11):1963–1972.
8. Ellingson BM, Chung C, Pope WB, Boxerman JL, Kaufmann TJ. Pseudoprogression, radionecrosis, inflammation or true tumor progression? challenges associated with glioblastoma response assessment in an evolving therapeutic landscape. *J Neurooncol.* 2017;134(3):495–504.
9. Okada H, Weller M, Huang R, et al. Immunotherapy response assessment in neuro-oncology: a report of the RANO working group. *Lancet Oncol.* 2015;16(15):e534–e542.
10. Kwak JJ, Tirumani SH, Van den Abbeele AD, Koo PJ, Jacene HA. Cancer immunotherapy: imaging assessment of novel treatment response patterns and immune-related adverse events. *Radiographics.* 2015;35(2):424–437.
11. Ellingson BM, Sampson J, Achrol AS, et al. Modified RANO, immunotherapy RANO, and standard RANO response to convection-enhanced delivery of IL4R-targeted immunotoxin MDNA55 in recurrent glioblastoma. *Clin Cancer Res.* 2021;27(14):3916–3925.
12. Ellingson BM, Malkin MG, Rand SD, et al. Validation of functional diffusion maps (fDMs) as a biomarker for human glioma cellularity. *J Magn Reson Imaging.* 2010;31(3):538–548.
13. Chen L, Liu M, Bao J, et al. The correlation between apparent diffusion coefficient and tumor cellularity in patients: a meta-analysis. *PLoS One.* 2013;8(11):e79008.
14. Chenevert TL, Stegman LD, Taylor JM, et al. Diffusion magnetic resonance imaging: an early surrogate marker of therapeutic efficacy in brain tumors. *J Natl Cancer Inst.* 2000;92(24):2029–2036.
15. Ellingson BM, Cloughesy TF, Lai A, et al. Graded functional diffusion map-defined characteristics of apparent diffusion coefficients predict overall survival in recurrent glioblastoma treated with bevacizumab. *Neuro Oncol.* 2011;13(10):1151–1161.
16. Ellingson BM, Cloughesy TF, Zaw T, et al. Functional diffusion maps (fDMs) evaluated before and after radiochemotherapy predict

progression-free and overall survival in newly diagnosed glioblastoma. *Neuro Oncol.* 2012;14(3):333–343.

17. Patel KS, Everson RG, Yao J, et al. Diffusion magnetic resonance imaging phenotypes predict overall survival benefit from bevacizumab or surgery in recurrent glioblastoma with large tumor burden. *Neurosurgery.* 2020;87(5):931–938.

18. Ellingson BM, Cloughesy TF, Lai A, Nghiemphu PL, Liau LM, Pope WB. Quantitative probabilistic functional diffusion mapping in newly diagnosed glioblastoma treated with radiochemotherapy. *Neuro Oncol.* 2013;15(3):382–390.

19. Pope WB, Qiao XJ, Kim HJ, et al. Apparent diffusion coefficient histogram analysis stratifies progression-free and overall survival in patients with recurrent GBM treated with bevacizumab: a multi-center study. *J Neurooncol.* 2012;108(3):491–498.

20. Song J, Kadaba P, Kravitz A, et al. Multiparametric MRI for early identification of therapeutic response in recurrent glioblastoma treated with immune checkpoint inhibitors. *Neuro Oncol.* 2020;22(11):1658–1666.

21. Mong S, Ellingson BM, Nghiemphu PL, et al. Persistent diffusion-restricted lesions in bevacizumab-treated malignant gliomas are associated with improved survival compared with matched controls. *AJNR Am J Neuroradiol.* 2012;33(9):1763–1770.

22. Ellingson BM, Kim HJ, Woodworth DC, et al. Recurrent glioblastoma treated with bevacizumab: contrast-enhanced T1-weighted subtraction maps improve tumor delineation and aid prediction of survival in a multicenter clinical trial. *Radiology.* 2014;271(1):200–210.

23. Ellingson BM, Kim E, Woodworth DC, et al. Diffusion MRI quality control and functional diffusion map results in ACRIN 6677/RTOG 0625: a multicenter, randomized, phase II trial of bevacizumab and chemotherapy in recurrent glioblastoma. *Int J Oncol.* 2015;46(5):1883–1892.

24. Sasaki M, Yamada K, Watanabe Y, et al.; Acute Stroke Imaging Standardization Group-Japan (ASIST-Japan) Investigators. Variability in absolute apparent diffusion coefficient values across different platforms may be substantial: a multivendor, multi-institutional comparison study. *Radiology.* 2008;249(2):624–630.

25. Yushkevich PA, Piven J, Hazlett HC, et al. User-guided 3D active contour segmentation of anatomical structures: significantly improved efficiency and reliability. *Neuroimage.* 2006;31(3):1116–1128.

26. Hagiwara A, Fujita S, Ohno Y, Aoki S. Variability and standardization of quantitative imaging: monoparametric to multiparametric quantification, radiomics, and artificial intelligence. *Invest Radiol.* 2020;55(9):601–616.

27. Ellingson BM, Gerstner ER, Smits M, et al. Diffusion MRI phenotypes predict overall survival benefit from anti-VEGF monotherapy in recurrent glioblastoma: converging evidence from phase II trials. *Clin Cancer Res.* 2017;23(19):5745–5756.

28. Cloughesy TF, Mochizuki AY, Orpilla JR, et al. Neoadjuvant anti-PD-1 immunotherapy promotes a survival benefit with intratumoral and systemic immune responses in recurrent glioblastoma. *Nat Med.* 2019;25(3):477–486.

29. Sugahara T, Korogi Y, Kochi M, et al. Usefulness of diffusion-weighted MRI with echo-planar technique in the evaluation of cellularity in gliomas. *J Magn Reson Imaging.* 1999;9(1):53–60.

30. Gupta RK, Cloughesy TF, Sinha U, et al. Relationships between choline magnetic resonance spectroscopy, apparent diffusion coefficient and quantitative histopathology in human glioma. *J Neurooncol.* 2000;50(3):215–226.

31. Patel KS, Yao J, Raymond C, et al. Decorin expression is associated with predictive diffusion MR phenotypes of anti-VEGF efficacy in glioblastoma. *Sci Rep.* 2020;10(1):14819.

32. Järveläinen H, Sainio A, Wight TN. Pivotal role for decorin in angiogenesis. *Matrix Biol.* 2015;43:15–26.

33. Huse M. Mechanical forces in the immune system. *Nat Rev Immunol.* 2017;17(11):679–690.

34. Merline R, Schaefer RM, Schaefer L. The matricellular functions of small leucine-rich proteoglycans (SLRPs). *J Cell Commun Signal.* 2009;3(3-4):323–335.

35. Elson A, Bovi J, Siker M, Schultz C, Paulson E. Evaluation of absolute and normalized apparent diffusion coefficient (ADC) values within the post-operative T2/FLAIR volume as adverse prognostic indicators in glioblastoma. *J Neurooncol.* 2015;122(3):549–558.

36. Rodriguez Gutierrez D, Manita M, Jaspan T, Dineen RA, Grundy RG, Auer DP. Serial MR diffusion to predict treatment response in high-grade pediatric brain tumors: a comparison of regional and voxel-based diffusion change metrics. *Neuro Oncol.* 2013;15(8):981–989.

37. Qin L, Li A, Qu J, et al. Normalization of ADC does not improve correlation with overall survival in patients with high-grade glioma (HGG). *J Neurooncol.* 2018;137(2):313–319.

38. Walker AJ, Ruzevick J, Malayeri AA, et al. Postradiation imaging changes in the CNS: how can we differentiate between treatment effect and disease progression? *Future Oncol.* 2014;10(7):1277–1297.